MODELLING ROTOR-ROTOR INTERACTION ON REDUCED PASSAGE COUNTS USING A TIME-DOMAIN FOURIER APPROACH

S.C. Stapelfeldt - L. di Mare

Mechanical Engineering Department, Imperial College London, London, United Kingdom,
sina.stapelfeldt05@imperial.ac.uk, l.di.mare@imperial.ac.uk

ABSTRACT

Blade row interaction is known to significantly affect aerodynamic performance and aeromechanical stability. Multi-stage flows can be modelled accurately on the whole annulus multi-stage domain. However, full circumference time-accurate simulations remain expensive and unpractical in the design cycle. This paper uses a time-domain Fourier based method to model steady and unsteady interaction effects in a 1.5 stage compressor. The method was developed for general non-axisymmetric flows across multiple blade rows. The computational domain includes several passages which are distributed over one wavelength of the fundamental stationary disturbance and act as sampling points for a circumferential Fourier transform. Flow variables at the pitch-wise boundaries and inlet/exit surfaces are updated from circumferential and temporal Fourier approximations. Results from the reduced passage model and whole annulus solutions are compared in terms of unsteady and time-averaged loads. The results demonstrate that the time-domain Fourier approach is capable of capturing steady and unsteady blade row interaction effects.

NOMENCLATURE

M	total number of spinning modes	N_K	number of circumferential harmonics
N_L	number of travelling disturbances	N_P	number of passages
N_R/N_S	rotor/stator blade count	N_T	number of time steps per period
P	pressure	P_{01}	inlet stagnation pressure
P_{datum}	passage averaged pressure	ΔP	amplitude of pressure perturbation
U	vector of conservation variables	$\bar{U}_0$	time-space average
U'	unsteady variation	$\tilde{U}$	circumferential variation
$\hat{U}$	Fourier coefficients	k	circumferential wavenumber
n	time step	s	surface coordinate
t	time	$\mathbf{x} = (x, r, \zeta)$	cylindrical coordinate vector
ζ	local circumferential coordinate	θ	global circumferential coordinate
μ	spinning mode index	σ_μ	unsteady contribution of mode μ
ϕ	phase of unsteady perturbation	Φ	phase of stationary perturbation
v	angular velocity	ω	angular frequency
Ω	wheel speed	ND	Nodal diameter
NGV	Nozzle guide vane	FULL	full circumference model
PS/SS	pressure/suction side	SPRS	sparse assembly model

INTRODUCTION

Unsteady 3D multi-stage flows can be modelled accurately by solving the flow governing equations on the whole circumference, multi-row domain. However, due to the large computational effort required for time-accurate computations, much of the design work is still based on steady flow calcu-

lations. Although sophisticated steady flow methods like the 'average-passage' model by Adamczyk (1985) take into account blade row interaction effects, they are inherently unsuitable for aeroelasticity calculations which require a time-accurate representation of unsteady flows. Hence, significant progress has been made over recent decades in the development of efficient unsteady methods in the time or frequency domain. Most of these techniques take advantage of the chorochronic periodicity inherent to turbomachines in order to solve the flow governing equations on a reduced number of passages.

The first single-passage method for forced response and flutter prediction in the time-domain was developed by Erdos et al. (1977). This 'direct store method' collects time histories at a periodic boundary and corrects conditions at the opposite boundary according to the phase-shifted periodicity. A disadvantage of this approach is that it requires large amounts of memory - particularly for large wavelength disturbances. He (1990) tackled this issue by following a similar approach but storing only the Fourier components of the flow variables at the pitchwise boundaries. This method was later extended to deal with multiple fundamental frequencies (He, 1992) and multiple blade rows (Dewhurst and He, 2000). Since the Fourier transform requires numerical integration over at least one period of the flow disturbance these methods are impractical for large wavelength disturbances. Gerolymos et al. (2002) improved convergence by introducing a moving averages technique to continuously update the Fourier coefficients at the pitchwise boundaries and blade row interfaces.

While all these methods accurately model stator-rotor or rotor-stator interference, limitations apply to the representation of interactions between more than two blade rows. Unequal blade counts of rows in the same frame of reference create circumferential non-uniformities in the time-averaged flow which cannot be captured by single passage methods as no temporal phase-shifted periodicity exists.

More recently, time-domain Fourier methods have been developed which adequately represent steady and unsteady flows with stationary circumferential variations. He (2006) accurately modelled inlet distortions and OGV-Pylon interaction by performing computations on multiple passages which are uniformly spaced across the circumference. The approach resembles the shape correction method with the additional approximation of the circumferential variation by a spatial Fourier transform. The spatial Fourier model has also been applied to non-axisymmetric unsteady flows in rotor disc cavities (He, 2011) and results in significant computational savings compared to whole annulus computations. The current paper extends the time-space Fourier approach to multi-stage flows. To the authors' knowledge, it presents the first application of a time-accurate reduced-passage method to rotor-rotor/stator-stator interaction and embedded row forcing.

METHODOLOGY

Flow Solver

The methodology is implemented in a finite-volume compressible flow solver which models the 3D unsteady Reynolds-averaged Navier-Stokes (URANS) equations. It thus assumes that only time-resolved unsteadiness is of interest and that the corresponding frequencies are far removed from the frequencies of turbulent flow structures. The turbulent eddy viscosity is evaluated using the Spalart-Allmaras model (Spalart and Allmaras, 1992). The solver stores flow variables at the nodes of a generic semi-structured grid. Numerical fluxes are computed along the grid edges using Roe's flux vector difference splitting coupled to Jameson's pressure switch to prevent the appearance of numerical oscillations. The solution method is implicit with second order accuracy in space and time. Local time stepping advances the solution in pseudo time for steady state computations. Unsteady computations use dual time stepping to ensure stability at high Courant numbers. A detailed description of the scheme can be found in Sayma et al. (2000).

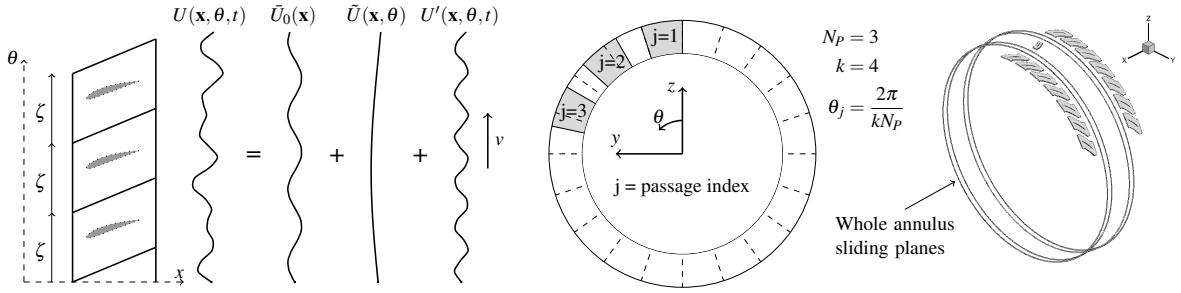

(a) Flow field decomposition

(b) Reduced passage domains (Left: Single-row domain for 4ND disturbance, Right: Multi-row domain)

Figure 1: **Schematics of sparse assembly domains**

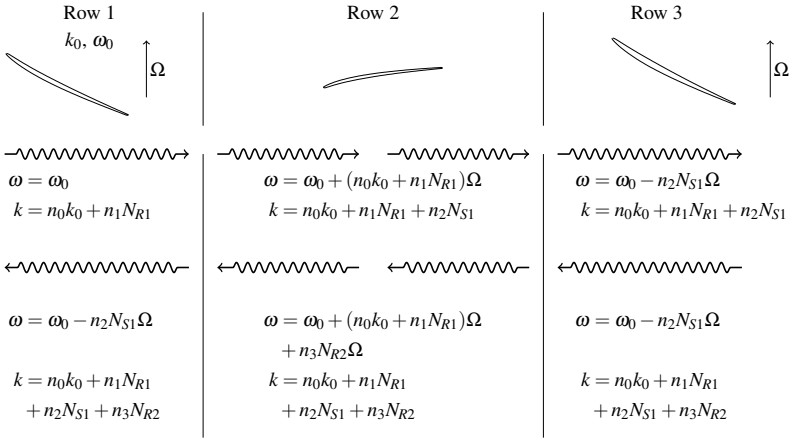

Figure 2: **Spinning modes**

Expression of Chorochronic Periodicity

The following methodology is based on the assumption that the flow variables at the periodic boundaries can be expressed as a superposition of a space-time average $\bar{U}_0(\mathbf{x})$, a stationary circumferential variation $\tilde{U}(\mathbf{x},\theta)$ and an unsteady contribution $U'(\mathbf{x},\theta,t)$ as illustrated in Figure 1a.

$$U(\mathbf{x},t) = \bar{U}_0(\mathbf{x}) + U'(\mathbf{x},\theta,t) + \tilde{U}(\mathbf{x},\theta) \tag{1}$$

Note that the vector $\mathbf{x} = (x, r, \zeta)$ describes the local coordinate system inside the passage with the circumferential coordinate ζ referenced to the blade, while θ is the global circumferential coordinate. Every point on the periodic boundary has thus got a different space-time average. Similarly, the unsteady and stationary fluctuation may vary in amplitude and phase inside the single passage domain due to the interaction with the steady flow field.

We furthermore assume that the unsteadiness is of 'deterministic' nature and periodic with a frequency related to the shaft frequency. Other sources of periodic unsteadiness, e.g. vortex shedding, are considered insignificant compared to the periodic fluctuations due to blade motion. The unsteadiness can then be described as a travelling wave with constant angular velocity v and angular frequency ω and a phase-lagged periodicity exists between adjacent passages. For blade row interaction problems, the frequency and wavelength of this unsteadiness are determined by the rotational speed and blade count of adjacent blade rows.

In absence of a stationary disturbance $\tilde{U}(\mathbf{x},\theta) = 0$ and $U'(\mathbf{x},\theta,t) = U'(\mathbf{x},t)$, i.e. the time-average and unsteady perturbation is the same in each passage and a time-space periodicity exists between adjacent passages. If more than one of these perturbations is present, the unsteady fluctuation can be

described as a superposition of N_L independent disturbances:

$$U'(\mathbf{x},\theta,t) = \sum_{l=1}^{N_L} U'_l(\mathbf{x},\theta,t) \tag{2}$$

where $U'_l(\mathbf{x},\theta,t)$ is the unsteady part of the l^{th} perturbation. The number of independent disturbances depends on the nature of the flow: For flows without strong interactions the independent disturbances are the fundamental perturbations at the source of the problem (e.g. travelling distortions, oscillating blades or blade row interactions). For flows with significant interactions the induced perturbations should also be included.

It then becomes possible to decompose the unsteadiness into the sum of its temporal Fourier components:

$$U'(\mathbf{x},t) = \sum_{l=1}^{N_L} \hat{U}_l(\mathbf{x}) e^{i(\frac{\omega_l}{v_l}\theta - \omega_l t)} \tag{3}$$

where, for conciseness, higher harmonics are included in summation over N_L. At every time step n the temporal Fourier coefficients are updated by applying a correction to those of the previous time step (Gerolymos et al., 2002).

$$\hat{U}(\mathbf{x})|_n = \hat{U}(\mathbf{x})|_{n-1} + \frac{1}{N_T}[(U(\mathbf{x},t_n) - U_n(\mathbf{x},t_n))e^{-i(\frac{\omega_l}{v_l}\theta - \omega_l t_n)}] \tag{4}$$

where $U_n(\mathbf{x},t_n)$ is the approximation of the flow variables at the current time step based on the Fourier coefficients of the previous time step and N_T is the number of time steps per period of the disturbance. The use of absolute phase angles in the Fourier transform and reconstruction ensures that points on the opposite boundary are updated with the correct phase lag.

So far it was assumed that the time-average flow does not vary from passage to passage. If a stationary disturbance with circumferential wavenumber k is superimposed onto a steady flow, the circumferential variation of the time-averaged flow $\tilde{U}(\mathbf{x},\theta)$ can be approximated by:

$$\tilde{U}(\mathbf{x},\theta) = \sum_{m=1}^{N_K} \hat{U}_m(\mathbf{x}) e^{i(mk\theta)} \tag{5}$$

The spatial Fourier coefficients $\hat{U}_m$ are evaluated by summation over N_P passages distributed over $1/k^{th}$ of the circumference (see Figure 1b). A 'reduced passage' or 'sparse assembly' domain with N_P spatial sampling points allows a Fourier approximation of order $(N_P-1)/2$.

$$\hat{U}_m(\mathbf{x}) = \frac{1}{N_P}\sum_{j=1}^{N_P} \tilde{U}(\mathbf{x},\theta) e^{-i(mk\theta)} \tag{6}$$

As with the travelling disturbances, the interaction of a single stationary disturbance with the time-space averaged flow field manifests itself in different amplitudes and phases inside the single passage domain.

Finally, we consider a flow where a stationary disturbance with circumferential wavenumber k interacts with an unsteady flow field. It can no longer be assumed that the temporal Fourier coefficients are uniform from passage to passage as the travelling wave may become distorted in the circumferential direction. The l^{th} travelling disturbance then takes the shape:

$$U'(\mathbf{x},\theta,t) = \sum_{l=1}^{N_L} \hat{U}_l(\mathbf{x},\theta) e^{-i(\frac{\omega_l}{v_l}\theta - \omega_l t)} \tag{7}$$

Similary to the stationary disturbance, we can approximate the circumferential variation of $\hat{U}_l(\mathbf{x},\theta)$ from a spatial Fourier transform:

$$\hat{U}_l(\mathbf{x},\theta) = \sum_{m=1}^{N_K} \hat{\hat{U}}_{lm}(\mathbf{x}) e^{-i(mk\theta)} \tag{8}$$

where the Fourier coefficients in time and space $\hat{\hat{U}}_{lm}(\mathbf{x})$ are evaluated from:

$$\hat{\hat{U}}_{lm}(\mathbf{x})|_n = \hat{\hat{U}}_{lm}(\mathbf{x})|_{n-1} + \frac{1}{N_T N_P} \sum_{j=1}^{N_P} [(U(\mathbf{x},\theta,t_n) - U_n(\mathbf{x},\theta,t_n)) e^{-i(km\theta + \frac{\omega_l}{v_l}\theta - \omega_l t_n)}] \tag{9}$$

Substituting back into Equation 7, it becomes possible to approximate the full variation in time and space.

$$U(\mathbf{x},\theta,t) = \sum_{l=0}^{N_L} \sum_{m=0}^{N_K} \hat{\hat{U}}_{l,m}(\mathbf{x}) e^{i(km\theta + \frac{\omega_l}{v_l}\theta - \omega_l t)} \tag{10}$$

Note that the approximations for the steady circumferential disturbance and undistorted travelling waves are recovered by $l = 0$ and $m = 0$ respectively.

Blade Row Interface Treatment

The circumferential and temporal variation of variables at the inter-row boundaries can be approximated in the same manner. Flow variables at the inlet or outlet boundaries are decomposed into spatial and temporal Fourier coefficients and a whole annulus image of the boundary surface can be reconstructed. The boundary conditions of the adjacent row are then interpolated from the whole annulus image. The interpolation procedure from the sliding plane onto the neighbouring row is identical to that used in whole annulus computations (Sayma et al., 2000).

Multi-stage Coupling

The independent frequencies N_L and the circumferential wave numbers k required for an accurate representation of multi-row interaction need to be determined. We refer to the theory of *spinning modes* or *Tyler-Sofrin modes* (Tyler and Sofrin, 1961) which desribes blade row interaction mechanisms through the scattering and frequency shifting of entropy, vorticity and pressure waves as they propagate between blade rows. Figure 2 shows the angular frequencies ω and circumferential wavenumbers k of a three-row compressor. Although, theoretically an infinite number of spinning modes exists, research has shown that in practice only a few modes contribute to the interrow coupling (e.g. Hall and Ekici, 2005).

In order to fully capture multi-stage coupling, the dominant spinning modes need to be approximated by the circumferential and temporal Fourier transform. Consider a rotor-stator-rotor configuration with N_{R1}, N_{S1} and N_{R2} blades respectively. If none of the blades vibrate, i.e. $k_0 = 0$ and $\omega_0 = 0$, the unsteady perturbations in the rotor domain are all multiples of the stator blade passing frequency $-n_2 N_{S1}\Omega$. The stator domain, on the other hand, sees linear combinations of the two rotor blade passings, i.e. waves with circumferential wave numbers $n_1 N_{R1} + n_3 N_{R2}$ travelling at rotational speed Ω.

Modes which satisfy $v = \omega/k$ need to be specified as distinctive travelling disturbances in Equation 10. The scattering of these modes through the local flow field is then accounted for in the circumferential Fourier transform or through the interaction with the local flow field. For example, consider mode $(n_1, n_2, n_3) = (1, 1, -1)$ in Rotor 1. This corresponds to a travelling wave with circumferential

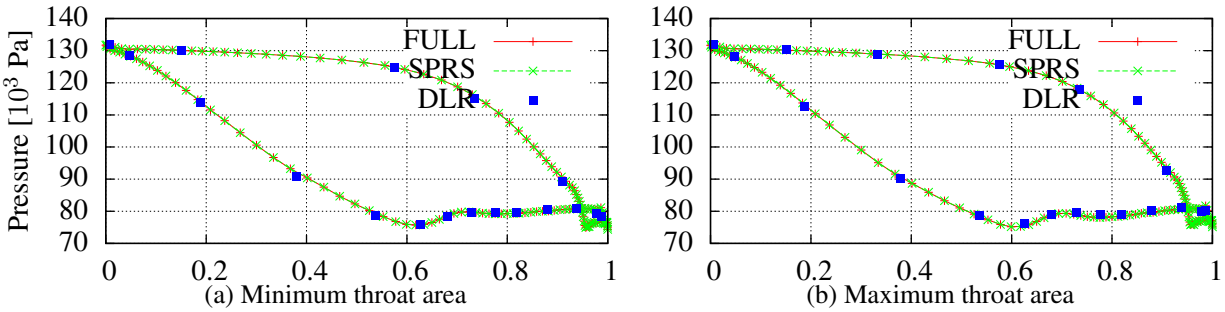

(a) Minimum throat area (b) Maximum throat area

Figure 3: **Comparison of NGV surface pressures at 50% span**

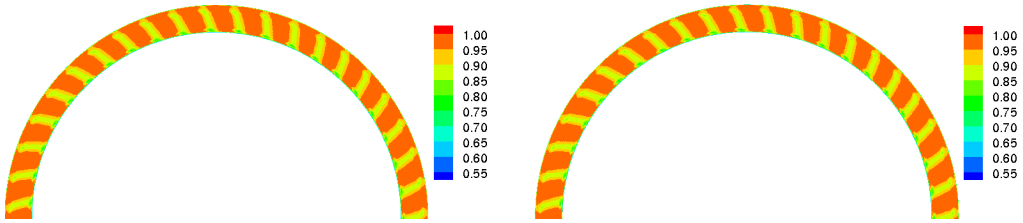

(a) Full circumference model (b) Reconstruction from sparse assembly

Figure 4: **Stagnation pressure contours at NGV outlet (non-dimensionalised by inlet pressure)**

wave number $n_2 N_{S1}$ and rotational velocity $-\Omega$ being modulated by a stationary disturbance with circumferential wavenumber $N_{R1} - N_{R2}$. It can therefore be fully represented by the circumferential variation of the temporal Fourier coefficients described previously, if the stationary disturbance due to the rotor-rotor interaction, i.e. wavenumber $N_{R1} - N_{R2}$, can be represented.

VALIDATION

NGV with throat area variation

Before an attempt at the unsteady modelling of rotor-stator-rotor interaction is made, the methodology and baseline flow solver are validated on a high pressure turbine. The turbine was designed for the European Collaborative Project "Aeroelastic Design of Turbine Blades II" which investigated sources of LEO excitation in turbines (Elliot et al., 2005). For the initial validation, a steady NGV-only case with moderate throat area variation is selected. The operating conditions are subsonic with downstream isentropic Mach number 0.85, inlet stagnation pressure 132kPa and pressure ratio 1.05. The throat area variation follows a sinusoidal 5ND pattern with maximum deviation of 4%. On the reduced passage model, this variation is represented on 5 discrete passages distributed over 72°. The passages are topologically equivalent and each blade is shifted to match the rig spacing pattern. The results are compared to the equivalent full circumference solution and rig measurements undertaken at DLR in 2002 (Rehder et al., 2002). Figure 3 shows the blade pressure profiles at 50% span for the blades with minimum and maximum throat area respectively. The blade pressure predictions of the flow solver match the experimental measurements and a very good agreement between the full circumference and reduced passage prediction exists. The full circumference and sparse assembly model are also compared in Figure 4 which shows the stagnation pressure contours at 130% chord non-dimensionalised by the inlet stagnation pressure. A more detailed comparison between the two models including rotor-stator interaction was presented in Stapelfeldt and di Mare (2012).

1.5 stage compressor

The multi-stage capabilities of the time-domain Fourier method are validated on a 1.5 stage compressor. In order to reduced computational requirements, only a thin section at mid-span is modelled. Performance parameters are listed in Table 2. If the blade counts are given by N_{R1}, N_{S1} and N_{R2} for

the first rotor, stator and second rotor respectively and $N_{R1} = N_{R2} + N_{aliased}$, the disturbances resulting from rotor-rotor interference has a circumferential wave number $N_{aliased}$. The interaction is modelled on seven passages per row which are distributed over the fundamental wavelength of the aliased disturbance. The embedded stator contains no stationary circumferential perturbation and a single passage is sufficient. Figure 1b shows the computational domain for the reduced passage model. Seven passages in the rotor domain allow a third order Fourier approximation of the rotor-rotor interaction. The unsteadiness is approximated from three harmonics per rotor/stator blade passing and the corresponding first 15 rotor-rotor interaction modes, i.e. the 15 modes with lowest wave number built from the linear combinations of $n_1 = (-3, -2, -1, 0, 1, 2, 3)$ and $n_3 = (-3, -2, -1, 0, 1, 2, 3)$. Note that modes $(n_1, 0, n_3)$ and $(-n_1, 0, -n_3)$ are complex conjugates and appear as the same disturbance in the stator.

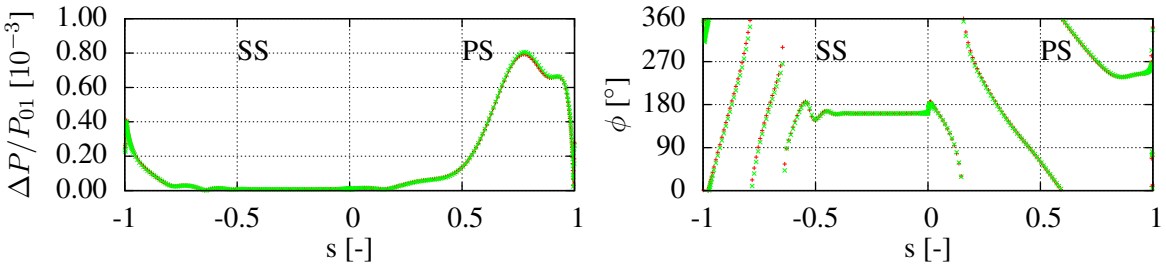

(a) **Rotor 1**

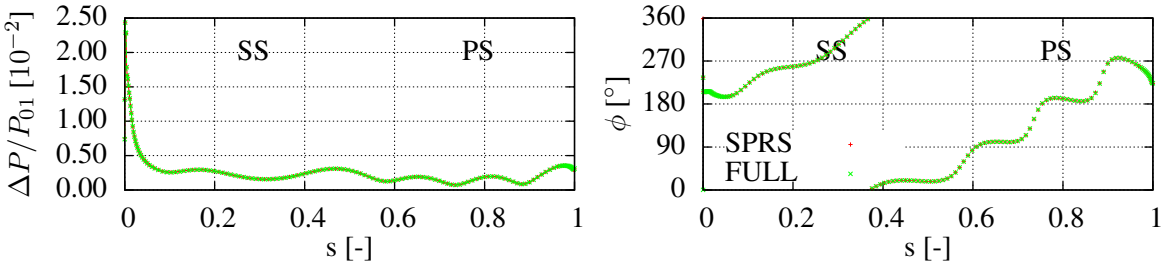

(b) **Rotor 2**

Figure 5: **Amplitude and phase of stator passing disturbance on rotor surface**

We aim to validate the reduced passage model by comparing the unsteady blade pressures to those predicted on the 360° domain. For this purpose, unsteady pressure histories on all sparse assembly blades are collected and post-processed. Post-processing Fourier transforms the histories in space and time and allows a reconstruction of instantaneous and time-averaged pressure profiles at arbitrary circumferential blade positions. Figure 5 compares blade pressures at the first blade ($\theta = 0$) of each rotor. Small differences between the two solutions are visible in amplitude and phase of the blade passing components but, overall, the two predictions are in good agreement. The unsteady pressure on the embedded stator is also well captured on the reduced-domain. This is illustrated in Figure 6, where the amplitude and phase of the upstream and downstream rotor passing frequency and their first linear combination are compared.

Figure 7 and Figure 8 compare the blade-to-blade (circumferential) variation of surface pressure as predicted by the whole annulus and the sparse assembly model. The variation of local pressure from the passage-averaged pressure is plotted against circumferential position for six locations on the blade surface (5%, 50% and 95% chord on the suction and pressure side). The circumferential position is expressed in terms of the phase of the aliased disturbance, such that 360° span the circumferential wavelength of the fundamental rotor-rotor interaction.

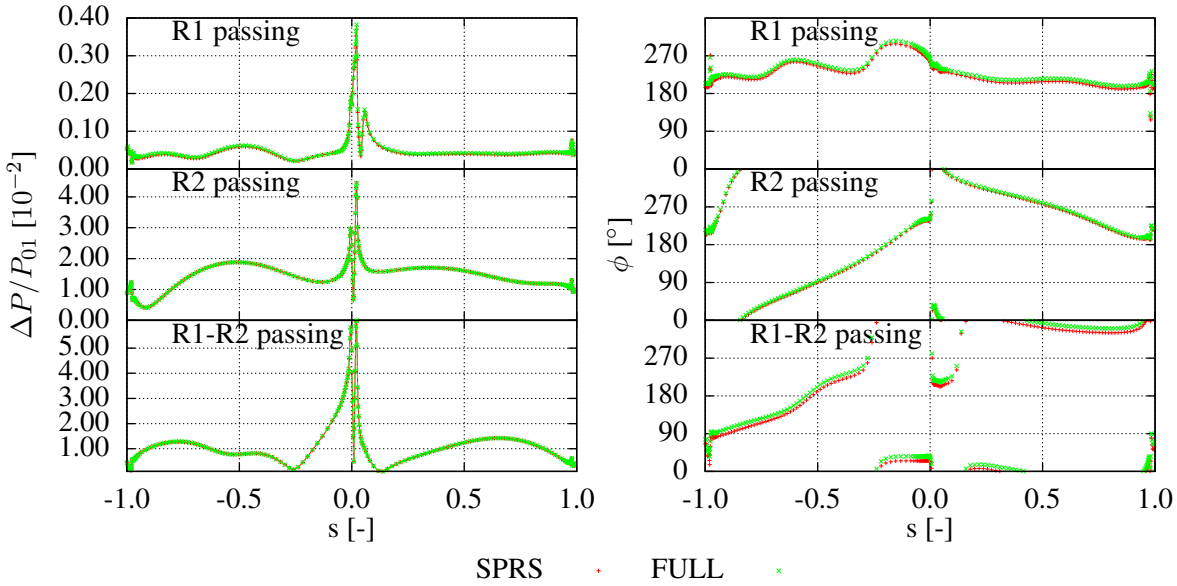

Figure 6: **Amplitude and phase of rotor passing disturbances on stator surface**

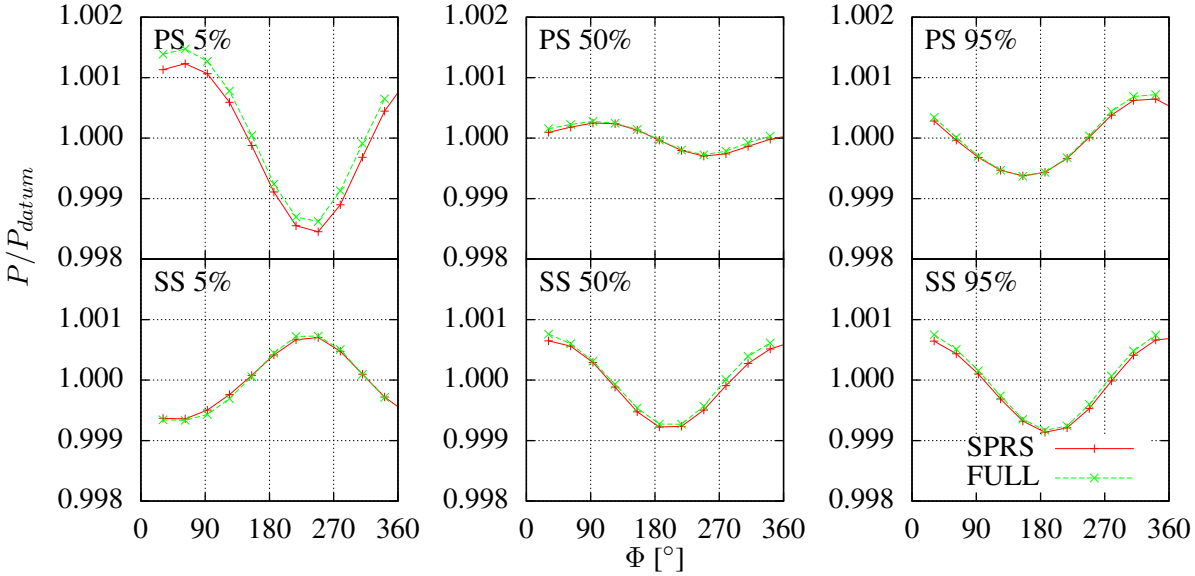

Figure 7: **R1 time-averaged pressure variation**

The effect of the downstream rotor on the upstream rotor is most noticeable in the pressure side leading edge region (PS 5% chord) where the maximum circumferential variation reaches approximately 0.2% of the average value. In the downstream direction, rotor-rotor interaction is stronger and more localised with a maximum variation of approximately 0.8% near the leading edge on the pressure side. Despite the relatively small blade-to-blade variations the reduced passage model reproduces the interaction pattern. In the downstream direction both amplitude and shape of the blade-to-blade variation are in good agreement. Differences between the two solutions are less than 2% of the maximum blade-to-blade variation in R2. In the upstream direction differences between the two solutions are more noticeable and locally reach up to 10% of the blade-to-blade variation.

In order to assess the relative importance of the travelling spinning modes specified in the stator domain, a time-space Fourier transform is carried out at mid-height in the stator outlet plane. The contribution of each mode μ to the total unsteadiness is then evaluated as $\sigma_\mu = \Delta P_\mu / \sum_\mu^M \Delta P_\mu$ where

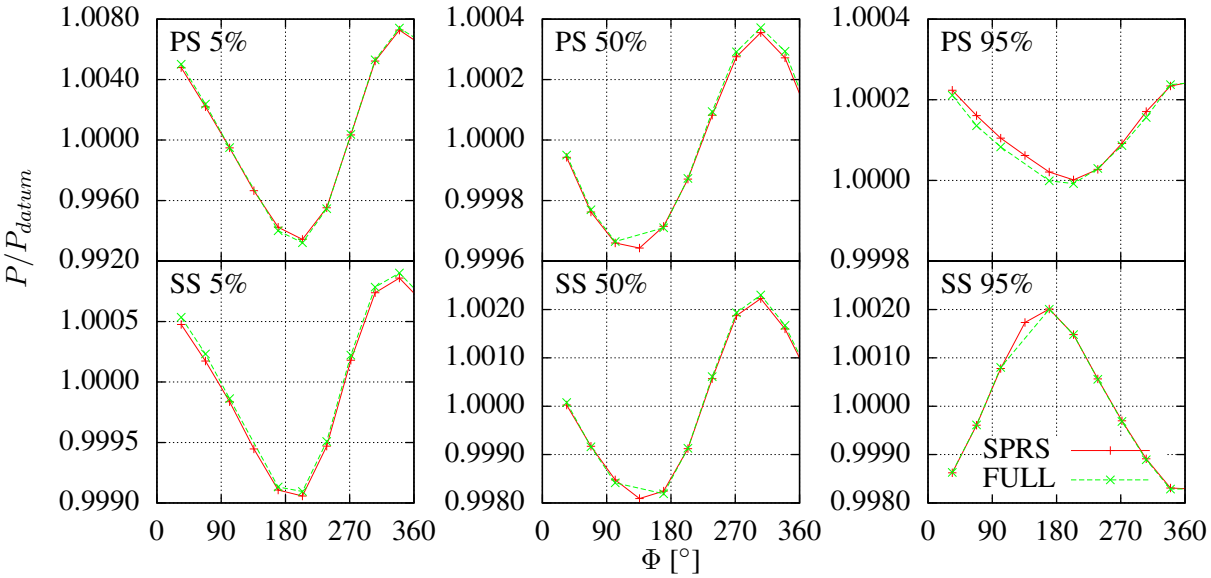

Figure 8: **R2 time-averaged pressure variation**

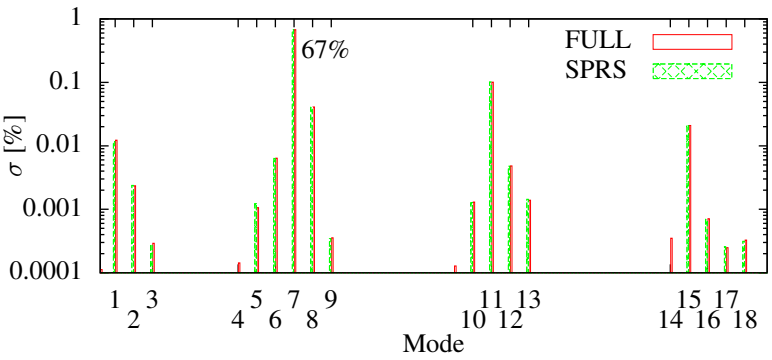

Mode	Wave number	Mode	Wave number
1	n_1-n_3	10	$-n_1+3n_3$
2	$2n_1-2n_3$	11	$2n_3$
3	$3n_1-3n_3$	12	n_1+n_3
4	$-3n_1+4n_3$	13	$2n_1$
5	$-2n_1+3n_3$	14	$-n_1+4n_1$
6	$-n_1+2n_3$	15	$3n_3$
7	n_3	16	n_1+2n_3
8	n_1	17	$2n_1+n_3$
9	$2n_1-n_3$	18	$3n_1$

Figure 9 & Table 1: **Contributions of travelling modes to total unsteadiness at stator outlet**

M is the total number of spinning modes detected at the stator outlet. Figure 9 shows the contribution of the first 12 travelling wave modes. The travelling waves make up 87% of the total unsteadiness with the second rotor blade passing frequency accounting for 67%. Figure 9 also illustrates that the high engine order sidebands (Modes 3, 5 and 10) are more than one order of magnitude lower than the first linear combination (Mode 1). This indicates that a similar level of accuracy could be achieved with three blade passing harmonics and fewer linear combinations of rotor-rotor passing frequencies.

Table 3 compares the grid dimensions and computational resources used for the two calculations. It must be noted, that the reduced passage model takes approximately two revolutions to reach a periodic state, while the full circumference model produces a converged solution after about 0.5 revolutions. Nevertheless, the sparse assembly reduces the total number of CPU-hours by a factor of 2-3. The benefits could be improved further by including fewer spinning modes in the computation.

CONCLUSIONS

This paper presented a time-domain Fourier method for the computation of unsteady flows in multi-stage turbomachinery. The method was validated on a rotor-stator-rotor configuration. Comparison of the reduced passage model with the whole annulus demonstrated that the method is capable of predicting steady rotor-rotor interaction and unsteady forcing on an embedded stator. The method is computationally efficient, requiring only a fraction of the size of the full circumference domain.

Flow coefficient	0.51
Load coefficient	0.52

Table 2: **Compressor operating conditions**

	SPRS	FULL
Grid points	300K	4M
CPUs	8	64
Revolutions	3	3
Wall clock time [h]	70	70

Table 3: **Grid size comparison**

ACKNOWLEDGEMENTS

The authors gratefully acknowledge Rolls-Royce plc for providing financial support toward this research and for giving permission to publish this paper.

REFERENCES

Adamczyk, J. J. (1985), '*Model Equation for Simulating Flows in Multistage Turbomachinery*', ASME Paper No. 85-GT-220 .

Dewhurst, S. and He, L. (2000), *Unsteady Flow Calculations Through Turbomachinery Stages Using Single Passage Domain With Shape Corrrection Method*, in '9th International Symposium on Unsteady Aerodynamics and Aeroelasticity in Turbomachines', Lyon, France.

Elliot, R., Green, J. S. and Seinturier, E. (2005), *Aeroelastic Design of Turbine Blades - AdTurBII Overview*, in '6th European Turbomachinery Conference', Lille, France.

Erdos, J. I., Alzner, E. and McNally, W. (1977), '*Numerical Solution of Periodic Transonic Flow Through a Fan Stage*', AIAA J **15**(11), 1559–1568.

Gerolymos, G. A., Michon, G. J. and Neubauer, J. (2002), '*Analysis and Application of Chorochronic Periodicity in Turbomachinery Rotor/Stator Interaction Computations*', J PROPUL POWER **18**(6), 1139–1152.

Hall, K. C. and Ekici, K. (2005), '*Multistage Coupling for Unsteady Flows in Turbomachinery*', AIAA J **43**(3), 624–632.

He, L. (1990), '*An Euler Solution for Unsteady Flows Around Oscillating Blades*', J TURBOMACH **112**(4), 714–722.

He, L. (1992), '*Method of Simulating Unsteady Turbomachinery Flows with Multiple Perturbations*', AIAA J **30**(11), 2730–2735.

He, L. (2006), '*Fourier Modelling of Nonaxisymmetrical Steady and Unsteady Flows*', J PROPUL POWER **22**(1), 197–201.

He, L. (2011), '*Efficient Computational Model for Nonaxisymmetric Flow and Heat Transfer in Rotating Cavity*', J TURBOMACH **133**(2), 021018–9.

Rehder, H.-J., Kost, F. and Kessar, A. (2002), Low Engine Order NGV Only Tests at DLR - Aeroelastic Design of Turbine Blades II, Technical Report ADTBII-DLR-WP2-2002, DLR.

Sayma, A. I., Vahdati, M. and Imregun, M. (2000), '*An Integrated Non Linear Approach for Turbomachinery Forced Response Prediction, Part 1: Formulation*', J FLUID STRUCT **14**(1), 87–101.

Spalart, P. R. and Allmaras, S. R. (1992), '*A One-Equation Turbulence Model for Aerodynamic Flows*', AIAA Paper 92-0439 .

Stapelfeldt, S. C. and di Mare, L. (2012), *Modelling flow past non-axisymmetric configurations on reduced passage counts*, in '13th International Symposium on Unsteady Aerodynamics, Aeroacoustics and Aeroelasticity in Turbomachinery', Tokyo, Japan.

Tyler, J. M. and Sofrin, T. G. (1961), '*Axial flow compressor noise studies*', SAE Transactions **70**, 309–332.